

Singapore Management University

## Institutional Knowledge at Singapore Management University

---

Research Collection School Of Computing and  
Information Systems

School of Computing and Information Systems

---

9-1996

### Strange $b$ baryon production and lifetime in $Z$ decays

D. BUSKULIC

M. THULASIDAS

*Singapore Management University*, [manojt@smu.edu.sg](mailto:manojt@smu.edu.sg)

Follow this and additional works at: [https://ink.library.smu.edu.sg/sis\\_research](https://ink.library.smu.edu.sg/sis_research)



Part of the [Databases and Information Systems Commons](#)

---

#### Citation

1

This Journal Article is brought to you for free and open access by the School of Computing and Information Systems at Institutional Knowledge at Singapore Management University. It has been accepted for inclusion in Research Collection School Of Computing and Information Systems by an authorized administrator of Institutional Knowledge at Singapore Management University. For more information, please email [cherylids@smu.edu.sg](mailto:cherylids@smu.edu.sg).



CERN-PPE/96-081

June 19, 1996

# Strange b baryon production and lifetime in Z decays

The ALEPH Collaboration

## Abstract

In a data sample of approximately four million hadronic Z decays recorded with the ALEPH detector from 1990 to 1995, a search for the strange b baryon  $\Xi_b$  is performed with a study of  $\Xi$ -lepton correlations. Forty-four events with same sign  $\Xi^- \ell^-$  combinations are found whereas 8.4 are expected based on the rate of opposite sign  $\Xi^- \ell^+$  combinations. This significant excess is interpreted as evidence for  $\Xi_b$  semileptonic decays. The measured product branching ratio is  $\text{Br}(b \rightarrow \Xi_b) \times \text{Br}(\Xi_b \rightarrow X_c X \ell^- \bar{\nu}) \times \text{Br}(X_c \rightarrow \Xi^- X') = (5.4 \pm 1.1(\text{stat}) \pm 0.8(\text{syst})) 10^{-4}$  per lepton species, averaged over electrons and muons, with  $X_c$  a charmed baryon. The  $\Xi_b$  lifetime is measured to be  $\tau_{\Xi_b} = 1.35^{+0.37}_{-0.28}(\text{stat})^{+0.15}_{-0.17}(\text{syst})$  ps.



a 1 9 9 6 0 0 1 a

(To be submitted to *Physics Letters B*)

# The ALEPH Collaboration

D. Buskulic, I. De Bonis, D. Decamp, P. Ghez, C. Goy, J.-P. Lees, A. Lucotte, M.-N. Minard, J.-Y. Nief, P. Odier, B. Pietrzyk

*Laboratoire de Physique des Particules (LAPP), IN<sup>2</sup>P<sup>3</sup>-CNRS, 74019 Annecy-le-Vieux Cedex, France*

M.P. Casado, M. Chmeissani, J.M. Crespo, M. Delfino, I. Efthymiopoulos,<sup>1</sup> E. Fernandez, M. Fernandez-Bosman, Ll. Garrido,<sup>15</sup> A. Juste, M. Martinez, S. Orteu, C. Padilla, I.C. Park, A. Pascual, J.A. Perlas, I. Riu, F. Sanchez, F. Teubert

*Institut de Fisica d'Altes Energies, Universitat Autònoma de Barcelona, 08193 Bellaterra (Barcelona), Spain<sup>7</sup>*

A. Colaleo, D. Creanza, M. de Palma, G. Gelao, M. Girone, G. Iaselli, G. Maggi,<sup>3</sup> M. Maggi, N. Marinelli, S. Nuzzo, A. Ranieri, G. Raso, F. Ruggieri, G. Selvaggi, L. Silvestris, P. Tempesta, G. Zito

*Dipartimento di Fisica, INFN Sezione di Bari, 70126 Bari, Italy*

X. Huang, J. Lin, Q. Ouyang, T. Wang, Y. Xie, R. Xu, S. Xue, J. Zhang, L. Zhang, W. Zhao

*Institute of High-Energy Physics, Academia Sinica, Beijing, The People's Republic of China<sup>8</sup>*

R. Alemany, A.O. Bazarko, G. Bonvicini,<sup>23</sup> M. Cattaneo, P. Comas, P. Coyle, H. Drevermann, R.W. Forty, M. Frank, R. Hagelberg, J. Harvey, P. Janot, B. Jost, E. Kneringer, J. Knobloch, I. Lehraus, G. Lutters, E.B. Martin, P. Mato, A. Minten, R. Miquel, Ll.M. Mir,<sup>2</sup> L. Moneta, T. Oest,<sup>20</sup> A. Pacheco, J.-F. Pusztazeri, F. Ranjard, P. Rensing,<sup>12</sup> L. Rolandi, D. Schlatter, M. Schmelling,<sup>24</sup> M. Schmitt, O. Schneider, W. Tejessy, I.R. Tomalin, A. Venturi, H. Wachsmuth, A. Wagner

*European Laboratory for Particle Physics (CERN), 1211 Geneva 23, Switzerland*

Z. Ajaltouni, A. Barrès, C. Boyer, A. Falvard, P. Gay, C. Guicheney, P. Henrard, J. Jousset, B. Michel, S. Monteil, J.-C. Montret, D. Pallin, P. Perret, F. Podlyski, J. Proriot, P. Rosnet, J.-M. Rossignol

*Laboratoire de Physique Corpusculaire, Université Blaise Pascal, IN<sup>2</sup>P<sup>3</sup>-CNRS, Clermont-Ferrand, 63177 Aubière, France*

T. Fearnley, J.B. Hansen, J.D. Hansen, J.R. Hansen, P.H. Hansen, B.S. Nilsson, B. Rensch, A. Wäänänen

*Niels Bohr Institute, 2100 Copenhagen, Denmark<sup>9</sup>*

A. Kyriakis, C. Markou, E. Simopoulou, I. Siotis, A. Vayaki, K. Zachariadou

*Nuclear Research Center Demokritos (NRCD), Athens, Greece*

A. Blondel, G. Bonneaud, J.C. Brient, P. Bourdon, A. Rougé, M. Rumpf, A. Valassi,<sup>6</sup> M. Verderi, H. Videau<sup>21</sup>

*Laboratoire de Physique Nucléaire et des Hautes Energies, Ecole Polytechnique, IN<sup>2</sup>P<sup>3</sup>-CNRS, 91128 Palaiseau Cedex, France*

D.J. Candlin, M.I. Parsons

*Department of Physics, University of Edinburgh, Edinburgh EH9 3JZ, United Kingdom<sup>10</sup>*

E. Focardi,<sup>21</sup> G. Parrini

*Dipartimento di Fisica, Università di Firenze, INFN Sezione di Firenze, 50125 Firenze, Italy*

M. Corden, C. Georgiopoulos, D.E. Jaffe

*Supercomputer Computations Research Institute, Florida State University, Tallahassee, FL 32306-4052, USA<sup>13,14</sup>*

A. Antonelli, G. Bencivenni, G. Bologna,<sup>4</sup> F. Bossi, P. Campana, G. Capon, D. Casper, V. Chiarella, G. Felici, P. Laurelli, G. Mannocchi,<sup>5</sup> F. Murtas, G.P. Murtas, L. Passalacqua, M. Pepe-Altarelli

*Laboratori Nazionali dell'INFN (LNF-INFN), 00044 Frascati, Italy*

L. Curtis, S.J. Dorris, A.W. Halley, I.G. Knowles, J.G. Lynch, V. O'Shea, C. Raine, P. Reeves, J.M. Scarr, K. Smith, P. Teixeira-Dias, A.S. Thompson, F. Thomson, S. Thorn, R.M. Turnbull

*Department of Physics and Astronomy, University of Glasgow, Glasgow G12 8QQ, United Kingdom<sup>10</sup>*

U. Becker, C. Geweniger, G. Graefe, P. Hanke, G. Hansper, V. Hepp, E.E. Kluge, A. Putzer, M. Schmidt, J. Sommer, H. Stenzel, K. Tittel, S. Werner, M. Wunsch

*Institut für Hochenergiephysik, Universität Heidelberg, 69120 Heidelberg, Fed. Rep. of Germany<sup>16</sup>*

D. Abbaneo, R. Beuselinck, D.M. Binnie, W. Cameron, P.J. Dornan, A. Moutoussi, J. Nash, J.K. Sedgbeer, A.M. Stacey, M.D. Williams

*Department of Physics, Imperial College, London SW7 2BZ, United Kingdom<sup>10</sup>*

G. Dissertori, P. Girtler, D. Kuhn, G. Rudolph

*Institut für Experimentalphysik, Universität Innsbruck, 6020 Innsbruck, Austria<sup>18</sup>*

A.P. Betteridge, C.K. Bowdery, P. Colrain, G. Crawford, A.J. Finch, F. Foster, G. Hughes, T. Sloan, M.I. Williams

*Department of Physics, University of Lancaster, Lancaster LA1 4YB, United Kingdom<sup>10</sup>*

A. Galla, I. Giehl, A.M. Greene, K. Kleinknecht, G. Quast, B. Renk, E. Rohne, H.-G. Sander, P. van Gemmeren, C. Zeitnitz

*Institut für Physik, Universität Mainz, 55099 Mainz, Fed. Rep. of Germany<sup>16</sup>*

J.J. Aubert,<sup>21</sup> A.M. Bencheikh, C. Benchouk, A. Bonissent, G. Bujosa, D. Calvet, J. Carr, C. Diaconu, F. Etienne, N. Konstantinidis, P. Payre, D. Rousseau, M. Talby, A. Sadouki, M. Thulasidas, K. Trabelsi

*Centre de Physique des Particules, Faculté des Sciences de Luminy, IN<sup>2</sup>P<sup>3</sup>-CNRS, 13288 Marseille, France*

M. Aleppo, F. Ragusa<sup>21</sup>

*Dipartimento di Fisica, Università di Milano e INFN Sezione di Milano, 20133 Milano, Italy*

I. Abt, R. Assmann, C. Bauer, W. Blum, H. Dietl, F. Dydak,<sup>21</sup> G. Ganis, C. Gotzhein, K. Jakobs, H. Kroha, G. Lütjens, G. Lutz, W. Männer, H.-G. Moser, R. Richter, A. Rosado-Schlosser, S. Schael, R. Settles, H. Seywerd, R. St. Denis, W. Wiedenmann, G. Wolf

*Max-Planck-Institut für Physik, Werner-Heisenberg-Institut, 80805 München, Fed. Rep. of Germany<sup>16</sup>*

J. Boucrot, O. Callot, Y. Choi,<sup>26</sup> A. Cordier, M. Davier, L. Duflot, J.-F. Grivaz, Ph. Heusse, A. Höcker, A. Jacholkowska, M. Jacquet, D.W. Kim,<sup>19</sup> F. Le Diberder, J. Lefrançois, A.-M. Lutz, I. Nikolic, H.J. Park,<sup>19</sup> M.-H. Schune, S. Simion, J.-J. Veillet, I. Videau, D. Zerwas

*Laboratoire de l'Accélérateur Linéaire, Université de Paris-Sud, IN<sup>2</sup>P<sup>3</sup>-CNRS, 91405 Orsay Cedex, France*

P. Azzurri, G. Bagliesi, G. Batignani, S. Bettarini, C. Bozzi, G. Calderini, M. Carpinelli, M.A. Ciocci, V. Ciulli, R. Dell'Orso, R. Fantechi, I. Ferrante, L. Foà,<sup>1</sup> F. Forti, A. Giassi, M.A. Giorgi, A. Gregorio, F. Ligabue, A. Lusiani, P.S. Marrocchesi, A. Messineo, F. Palla, G. Rizzo, G. Sanguinetti, A. Sciabà, P. Spagnolo, J. Steinberger, R. Tenchini, G. Tonelli,<sup>25</sup> C. Vannini, P.G. Verdini, J. Walsh

*Dipartimento di Fisica dell'Università, INFN Sezione di Pisa, e Scuola Normale Superiore, 56010 Pisa, Italy*

G.A. Blair, L.M. Bryant, F. Cerutti, J.T. Chambers, Y. Gao, M.G. Green, T. Medcalf, P. Perrado, J.A. Strong, J.H. von Wimmersperg-Toeller

*Department of Physics, Royal Holloway & Bedford New College, University of London, Surrey TW20 OEX, United Kingdom<sup>10</sup>*

D.R. Botterill, R.W. Clift, T.R. Edgecock, S. Haywood, P. Maley, P.R. Norton, J.C. Thompson, A.E. Wright

*Particle Physics Dept., Rutherford Appleton Laboratory, Chilton, Didcot, Oxon OX11 0QX, United Kingdom*<sup>10</sup>

B. Bloch-Devaux, P. Colas, S. Emery, W. Kozanecki, E. Lançon, M.C. Lemaire, E. Locci, B. Marx, P. Perez, J. Rander, J.-F. Renardy, A. Roussarie, J.-P. Schuller, J. Schwindling, A. Trabelsi, B. Vallage

*CEA, DAPNIA/Service de Physique des Particules, CE-Saclay, 91191 Gif-sur-Yvette Cedex, France*<sup>17</sup>

S.N. Black, J.H. Dann, R.P. Johnson, H.Y. Kim, A.M. Litke, M.A. McNeil, G. Taylor

*Institute for Particle Physics, University of California at Santa Cruz, Santa Cruz, CA 95064, USA*<sup>22</sup>

C.N. Booth, R. Boswell, C.A.J. Brew, S. Cartwright, F. Combley, A. Koksai, M. Letho, W.M. Newton, J. Reeve, L.F. Thompson

*Department of Physics, University of Sheffield, Sheffield S3 7RH, United Kingdom*<sup>10</sup>

A. Böhrer, S. Brandt, V. Büscher, G. Cowan, C. Grupen, J. Minguet-Rodriguez, F. Rivera, P. Saraiva, L. Smolik, F. Stephan,

*Fachbereich Physik, Universität Siegen, 57068 Siegen, Fed. Rep. of Germany*<sup>16</sup>

M. Apollonio, L. Bosisio, R. Della Marina, G. Giannini, B. Gobbo, G. Musolino

*Dipartimento di Fisica, Università di Trieste e INFN Sezione di Trieste, 34127 Trieste, Italy*

J. Rothberg, S. Wasserbaech

*Experimental Elementary Particle Physics, University of Washington, WA 98195 Seattle, U.S.A.*

S.R. Armstrong, P. Elmer, Z. Feng,<sup>27</sup> D.P.S. Ferguson, Y.S. Gao,<sup>28</sup> S. González, J. Grahl, T.C. Greening, O.J. Hayes, H. Hu, P.A. McNamara III, J.M. Nachtman, W. Orejudos, Y.B. Pan, Y. Saadi, I.J. Scott, A.M. Walsh,<sup>29</sup> Sau Lan Wu, X. Wu, J.M. Yamartino, M. Zheng, G. Zobernig

*Department of Physics, University of Wisconsin, Madison, WI 53706, USA*<sup>11</sup>

---

<sup>1</sup>Now at CERN, 1211 Geneva 23, Switzerland.

<sup>2</sup>Supported by Dirección General de Investigación Científica y Técnica, Spain.

<sup>3</sup>Now at Dipartimento di Fisica, Università di Lecce, 73100 Lecce, Italy.

<sup>4</sup>Also Istituto di Fisica Generale, Università di Torino, Torino, Italy.

<sup>5</sup>Also Istituto di Cosmo-Geofisica del C.N.R., Torino, Italy.

<sup>6</sup>Supported by the Commission of the European Communities, contract ERBCHBICT941234.

<sup>7</sup>Supported by CICYT, Spain.

<sup>8</sup>Supported by the National Science Foundation of China.

<sup>9</sup>Supported by the Danish Natural Science Research Council.

<sup>10</sup>Supported by the UK Particle Physics and Astronomy Research Council.

<sup>11</sup>Supported by the US Department of Energy, grant DE-FG0295-ER40896.

<sup>12</sup>Now at Dragon Systems, Newton, MA 02160, U.S.A.

<sup>13</sup>Supported by the US Department of Energy, contract DE-FG05-92ER40742.

<sup>14</sup>Supported by the US Department of Energy, contract DE-FC05-85ER250000.

<sup>15</sup>Permanent address: Universitat de Barcelona, 08208 Barcelona, Spain.

<sup>16</sup>Supported by the Bundesministerium für Forschung und Technologie, Fed. Rep. of Germany.

<sup>17</sup>Supported by the Direction des Sciences de la Matière, C.E.A.

<sup>18</sup>Supported by Fonds zur Förderung der wissenschaftlichen Forschung, Austria.

<sup>19</sup>Permanent address: Kangnung National University, Kangnung, Korea.

<sup>20</sup>Now at DESY, Hamburg, Germany.

<sup>21</sup>Also at CERN, 1211 Geneva 23, Switzerland.

<sup>22</sup>Supported by the US Department of Energy, grant DE-FG03-92ER40689.

<sup>23</sup>Now at Wayne State University, Detroit, MI 48202, USA.

<sup>24</sup>Now at Max-Planck-Institut für Kernphysik, Heidelberg, Germany.

<sup>25</sup>Also at Istituto di Matematica e Fisica, Università di Sassari, Sassari, Italy.

<sup>26</sup>Permanent address: Sung Kyun Kwon University, Suwon, Korea.

<sup>27</sup>Now at The Johns Hopkins University, Baltimore, MD 21218, U.S.A.

<sup>28</sup>Now at Harvard University, Cambridge, MA 02138, U.S.A.

<sup>29</sup>Now at Rutgers University, Piscataway, NJ 08855-0849, U.S.A.

# 1 Introduction

Significant progress has been made in the last decade in the study of B mesons. The detailed experimental study of the production rates and properties of the b baryons is more recent, made possible with the advent of the LEP and Tevatron experiments.

The production rate of b baryons at LEP is measured [1] to account for about 12% of b hadrons, dominated by the lightest state  $\Lambda_b$ , produced either directly or from  $\Sigma_b$  or  $\Sigma_b^*$  decays. Indirect evidence for the  $\Lambda_b$  was reported by the LEP experiments [2] from the study of  $\Lambda\ell^-$  and  $\Lambda_c^+\ell^-$  correlations. Later, the  $\Lambda_b$  lifetime [3] and  $\Lambda_b$  polarization [4] were measured. Direct evidence for the  $\Lambda_b$  [5] in exclusive hadronic decays was reported recently and its mass determined.

The strange b baryons  $\Xi_b$  and  $\Omega_b$  are expected to be produced in  $Z \rightarrow b\bar{b}$  decays<sup>1</sup>. The production of  $\Xi_b$  is more abundant than  $\Omega_b$  due to the lower number of constituent strange quarks in the  $\Xi_b$ . Ground state  $\Xi_b$  decays proceed as for  $\Lambda_b$  via weak decays. Following the same procedure used for the indirect search of  $\Lambda_b$  in hadronic Z decays, the  $\Xi_b$  baryons are searched for in the semileptonic decay channel, namely  $\Xi_b \rightarrow X_c X \ell^- \bar{\nu}_\ell$  followed by<sup>2</sup>  $X_c \rightarrow \Xi^- X$ , using the charge correlation between the  $\Xi^-$  and the lepton as a tag. Therefore the signature for  $\Xi_b$  decaying semileptonically is the presence of same sign  $\Xi^-\ell^-$  pairs. A first study of the production of strange b baryons in Z decays was recently published by the DELPHI collaboration [6].

## 2 The ALEPH Detector

The ALEPH detector and its performance are described in detail elsewhere [7]. In this section, only a brief description of the apparatus properties most relevant to this analysis is given. The critical elements are charged particle tracking, including especially the silicon vertex detector, particle identification with ionization energy loss ( $dE/dx$ ), electron identification in the electromagnetic calorimeter and muon identification in the hadronic calorimeter supplemented by muon chambers.

Charged particles are tracked with three concentric devices residing inside an axial magnetic field of 1.5 T. Just outside the 5.4 cm radius beam pipe is the vertex detector (VDET) [8], which consists of double sided silicon microstrip detectors with strip readout in two orthogonal directions. The strip detectors are arranged in two cylindrical layers at average radii of 6.3 and 10.8 cm, with solid angle coverage of  $|\cos\theta| < 0.85$  for the inner layer, and  $|\cos\theta| < 0.69$  for the outer layer. The point resolution for tracks at normal incidence is 12  $\mu\text{m}$  in both the  $r\phi$  and  $z$  projections.

Surrounding the VDET is the inner tracking chamber (ITC), a cylindrical drift chamber with up to eight measurements in the  $r\phi$  projection. Outside the ITC, the time projection chamber (TPC) provides up to 21 space points for  $|\cos\theta| < 0.79$ , and a decreasing number of measurements at smaller angles, with 4 space points at  $|\cos\theta| = 0.96$ .

The combined tracking system has a transverse momentum resolution of  $\Delta p_t/p_t = 0.0006 \times p_t \oplus 0.005$  ( $p_t$  in GeV/c). For tracks with hits in both VDET layers the impact parameter resolution on a track of momentum  $p$  is  $25 \mu\text{m} + 95 \mu\text{m}/p$  ( $p$  in GeV/c).

In addition to tracking, the TPC is used for particle identification by measurement of

<sup>1</sup>Throughout this paper,  $\Xi_b$  is used as a generic name for  $\Xi_b^0$  and  $\Xi_b^-$ ,  $\Xi_c$  for  $\Xi_c^0$  and  $\Xi_c^+$ , B for  $B^+$ ,  $B^0$  and  $B_s$  mesons, and D for  $D^+$ ,  $D^0$  and  $D_s$  mesons. Charge conjugate modes are implied everywhere.

<sup>2</sup> $X_c$  is used as a generic name for a charmed baryon which may give a  $\Xi$  hyperon in its decays:  $X_c$  is dominantly  $\Xi_c$  but may also be  $\Lambda_c^+$ ,  $\Sigma_c$  or  $\Omega_c$ .

the ionization energy loss associated with each charged track. It provides up to 338 dE/dx measurements, with a measured resolution of 4.5% for Bhabha electrons with at least 330 ionization samples. For charged particles with momenta above 3 GeV/c, the mean dE/dx gives a separation of approximately 3 standard deviations ( $\sigma$ ) between pions and protons. At least 50 ionisation samples are required to get a dE/dx measurement; this occurs for 80% of charged tracks.

Electrons are identified by their shower shape in the electromagnetic calorimeter (ECAL), a lead-proportional chamber sandwich segmented into 15 mrad  $\times$  15 mrad projective towers which are read out in three sections in depth. The dE/dx measurement on the track, if any, gives an independent signature for electrons. Muons are identified from their pattern in the hadron calorimeter (HCAL), a seven interaction length yoke interleaved with 23 layers of streamer tubes; two double layers of muon chambers outside the HCAL give an additional signature for muons.

### 3 Origin of $\Xi$ -lepton combinations in hadronic Z decays

There are five possible sources of  $\Xi$ -lepton combinations in hadronic Z decays :

$$\Xi_b \rightarrow X_c X \ell^- \bar{\nu}_\ell, \quad X_c \rightarrow \Xi^- X \quad (1)$$

$$(\Lambda_b, \bar{B}) \rightarrow X_c X \ell^- \bar{\nu}_\ell, \quad X_c \rightarrow \Xi^- X \quad (2)$$

$$b, c \rightarrow X_c X, \quad X_c \rightarrow \Xi^- \ell^+ X \nu_\ell \quad (3)$$

$$\text{Accidental combinations} \quad (4)$$

$$\text{Fake combinations} \quad (5)$$

Process (1) is the signal and leads to same sign  $\Xi^- \ell^-$  combinations. Process (2) also leads to same sign combinations. Process (3) leads to opposite sign  $\Xi^- \ell^+$  combinations only. Accidental combinations arise when a  $\Xi^-$  baryon from fragmentation is paired with a lepton from the semileptonic decay of a c or b hadron. Fake combinations (5) occur when a misidentified hadron (fake lepton) is paired with a true  $\Xi^-$ , or a lepton from the semileptonic decay of a c or b hadron with a fake  $\Xi^-$  (spurious  $\Lambda\pi$  combination with invariant mass compatible with the  $\Xi^-$  mass), or a fake lepton with a fake  $\Xi^-$ .

## 4 Strange b baryon candidate selection

### 4.1 The event sample

The analysis presented in this letter is based on about 4.2 million hadronic Z decays recorded with the ALEPH detector from 1990 to 1995 and selected as described in [9].

The Monte Carlo simulation is done with the JETSET 7.4 program using the LUND model [10] slightly modified to take into account the latest values of the decay branching fractions of c and b mesons and baryons. All the simulated events are processed through the chain of reconstruction and analysis programs used for the data. Five Monte Carlo data sets are used for this analysis, one for each process of section 3. For the signal, the simulated data consist of 40,000 decays  $\Xi_b \rightarrow \Xi_c X \ell^- \bar{\nu}_\ell$  with no polarisation, of 20,000 decays with 100%  $\Xi_b$  polarisation, and of a third set with  $\Xi_b \rightarrow \Xi_c \rho \ell^- \bar{\nu}_\ell$  for specific studies of four-body decays. For processes (2) and (3), different specific decay channels of  $\Lambda_b$ , B mesons,  $\Lambda_c^+$  and  $\Xi_c$  giving a  $\Xi^-$  and a lepton have been generated, with at least 3000 events per channel. For processes (4), a set of events with a  $\Xi^-$  and a lepton in the same event hemisphere equivalent

to 12 times the data sample has been generated. The estimation of fake combinations has been done on the standard ALEPH Monte Carlo data set, equivalent to 5.6 million hadronic Z decays.

## 4.2 $\Xi_b$ candidate selection

The event selection starts with the requirement of hadronic Z events where a  $\Xi^-$  is associated with a lepton in the same hemisphere with respect to the thrust axis. The lepton candidate selection is described in [11]. Electron and muon candidates are required to have a momentum greater than 3 GeV/c.

The  $\Xi^-$  candidates are reconstructed through their decay  $\Xi^- \rightarrow \Lambda \pi^-$ . The  $\Lambda$  candidates are reconstructed in the decay channel  $\Lambda \rightarrow p \pi^-$ , using a slightly modified version of the algorithm described in [12]. To reduce the combinatorial background, the two oppositely charged tracks are required to have a total momentum greater than 2.5 GeV/c and to form a vertex corresponding to a decay length of at least 5 cm from the interaction point. The dE/dx measurements of the two tracks, when available, are required to be within  $3\sigma$  of those expected for a proton and a pion respectively. To reduce the possible contamination from other displaced vertices, the invariant mass of the two daughter tracks is required to be within  $3\sigma$  of the  $\Lambda$  mass ( $\sigma$  is momentum-dependent, as described in [12], with an average value of 3 MeV/c<sup>2</sup>) and incompatible with the  $\gamma \rightarrow e^+e^-$  hypothesis ( $M_{e^+e^-} > 15$  MeV/c<sup>2</sup>). If the dE/dx information for the proton candidate is consistent with that of a pion, or if the dE/dx information is not available for the proton candidate, an additional cut to remove  $K_s^0$ 's is applied ( $|M_{\pi\pi} - M_{K_s^0}| > 10$  MeV/c<sup>2</sup>, i.e. a  $3\sigma$  cut around the  $K_s^0$  mass).

To reconstruct  $\Xi^-$  baryons, the selected  $\Lambda$  candidates are combined with a pion from the same hemisphere having a negative charge. The pion is required to have a transverse momentum between 0.09 and 0.2 GeV/c with respect to the  $\Lambda\pi^-$  system, to eliminate most of the  $\Lambda\pi^-$  combinatorial background. The  $\Lambda\pi^-$  system is required to have a momentum greater than 3 GeV/c and a longitudinal momentum with respect to the event thrust axis greater than 2.5 GeV/c. The  $\chi^2$  probability of the  $\Lambda\pi^-$  vertex fit must be greater than 1% and the  $\Lambda\pi^-$  decay length with respect to the interaction point must be greater than 1.5 cm. Finally, the  $\Lambda\pi^-$  system is required to satisfy  $|M_{\Lambda\pi} - M_{\Xi}| < 23$  MeV/c<sup>2</sup>, with  $M_{\Xi} = 1321.3$  MeV/c<sup>2</sup> from [13] and where 23 MeV/c<sup>2</sup> is equal to three times the typical  $\Xi^-$  mass resolution.

Selected  $\Xi^-$  candidates are combined with an identified lepton from the same hemisphere if the angle between the  $\Xi^-$  and the lepton is less than 30°. The  $\Xi^-$  and the lepton are required to belong to the same jet.<sup>3</sup> The  $\Xi$ -lepton system is required to have an invariant mass between 2.5 and 5.0 GeV/c<sup>2</sup>; this cut eliminates completely all combinations coming from semileptonic decays of charmed baryons.

Fig. 1 shows the  $\Lambda\pi^-$  invariant mass distribution of the same sign  $\Xi^-\ell^-$  and the opposite sign  $\Xi^-\ell^+$  combinations after all selection cuts are applied except the  $\Lambda\pi$  mass cut. A mass peak is seen in both distributions at the  $\Xi^-$  mass, with a clear excess of  $\Xi^-\ell^-$  with respect to  $\Xi^-\ell^+$  combinations. A fit to the two distributions (a Gaussian for the  $\Xi^-$  peak and a polynomial for the background) yields a mean value compatible with the nominal  $\Xi^-$  mass, and a width consistent with the Monte Carlo expectation (7.5 MeV/c<sup>2</sup>).

<sup>3</sup>The jets are defined with the JADE algorithm [14] with  $y_{\text{cut}} = 0.015$ .



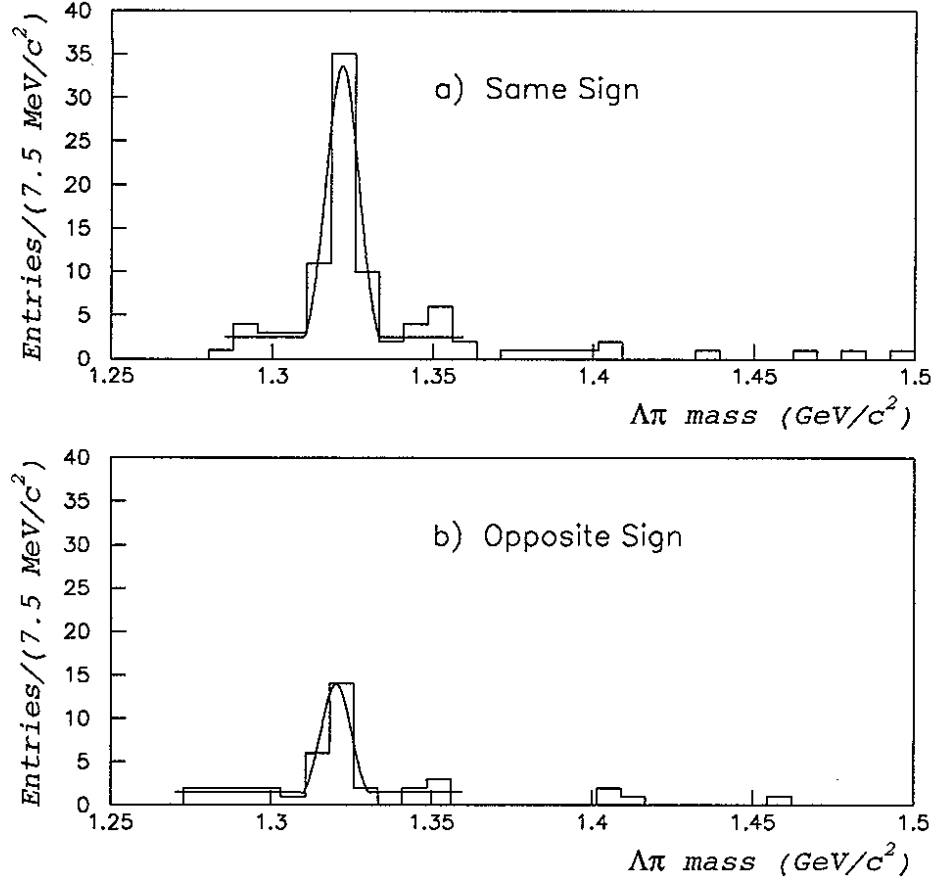


Figure 1: The  $\Lambda\pi^-$  invariant mass distribution of (a) the same sign  $\Xi^-\ell^-$  and (b) the opposite sign  $\Xi^-\ell^+$  combinations. All selection cuts of section 4.2 are applied except the  $\Lambda\pi^-$  mass cut. The curve is the result of a fit described in the text.

### 4.3 Improved $\Xi_b$ selection with a discriminating variable

To improve the  $\Xi_b$  purity in the final  $\Xi^-\ell^-$  sample, a set of five discriminating variables is used, following the method described in [15]. These variables are:

- $P_t(\Xi)$ , the longitudinal momentum of the  $\Xi^-$  with respect to the thrust axis;
- $P_t(\ell)$ , the transverse momentum of the lepton with respect to the jet containing the  $\Xi$ -lepton pair;
- $M(\Xi\ell)$ , the  $\Xi$ -lepton invariant mass;
- $P(\Xi\ell)$ , the  $\Xi$ -lepton momentum;
- $N_{\text{ch}}$ , the number of charged tracks in the jet.

The distributions of these variables are determined from the Monte Carlo signal data set (without polarisation) for the signal and from the set simulating processes (4) for background.

These distributions are normalized to unit area and fitted to build probability density functions (displayed in Fig. 2) for the five discriminating variables. The signal and background processes differ in each variable; however a clear separation of signal and

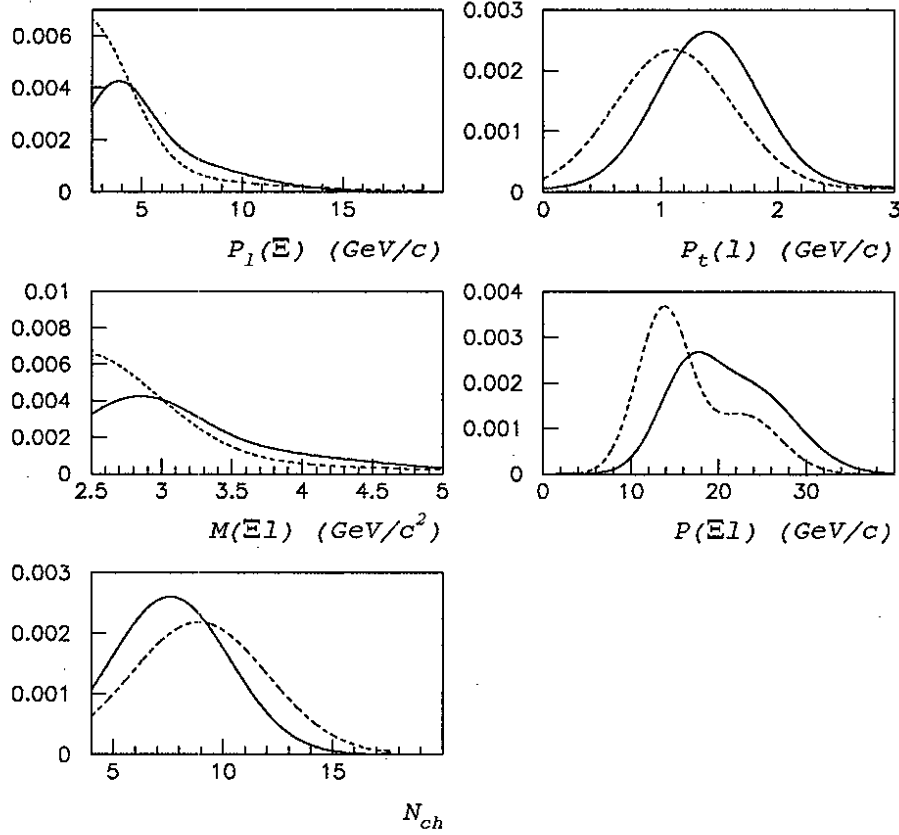


Figure 2: Probability density functions of the five discriminating variables used to build the global  $x_{\text{eff}}$  variable. Full lines : functions  $s_i(x_i)$  for the signal  $\Xi_b$  decays; Dashed lines : functions  $b_i(x_i)$  for the background.

background is not efficient in any single variable. Therefore, these five variables are combined into a single discriminating variable  $x_{\text{eff}}$  defined as follows [15]:

$$x_{\text{eff}} = \frac{\eta \prod_{i=1}^5 b_i(x_i)}{(1 - \eta) \prod_{i=1}^5 s_i(x_i) + \eta \prod_{i=1}^5 b_i(x_i)}$$

where  $s_i(x_i)$  and  $b_i(x_i)$  are the probability density functions for the discriminating variable  $x_i$  of the signal and background  $\Xi$ -lepton events respectively, and  $\eta$  is the expected fraction of background same sign  $\Xi^-\ell^-$  pairs. The value  $\eta = 0.45 \pm 0.15$  is determined from the ratio of opposite to same sign pairs in the data; this ratio is corrected by a factor  $1.2 \pm 0.2$  determined by the Monte Carlo to take into account the asymmetry of this background ( $\Lambda_b$  and B meson semileptonic decays contribute to same sign pairs and not to opposite sign pairs). The discriminating variables have been chosen to give a flat  $x_{\text{eff}}$  distribution for the background processes (3,4,5) of section 3, and a distribution peaked near 0 for the signal.

Fig. 3 shows the  $x_{\text{eff}}$  distributions for the same sign and the opposite sign  $\Xi$ -lepton pairs in data and Monte Carlo. The  $x_{\text{eff}}$  distribution is flat for  $\Xi^-\ell^+$  pairs and peaked at zero for  $\Xi^-\ell^-$  pairs coming from  $\Xi_b$  decays, allowing a clear discrimination between signal and background. In the following, all events with  $x_{\text{eff}} > 0.3$  are rejected. This value is chosen as a compromise between the efficiency of the analysis and the improvement of the  $\Xi_b$  purity in the same sign pairs.

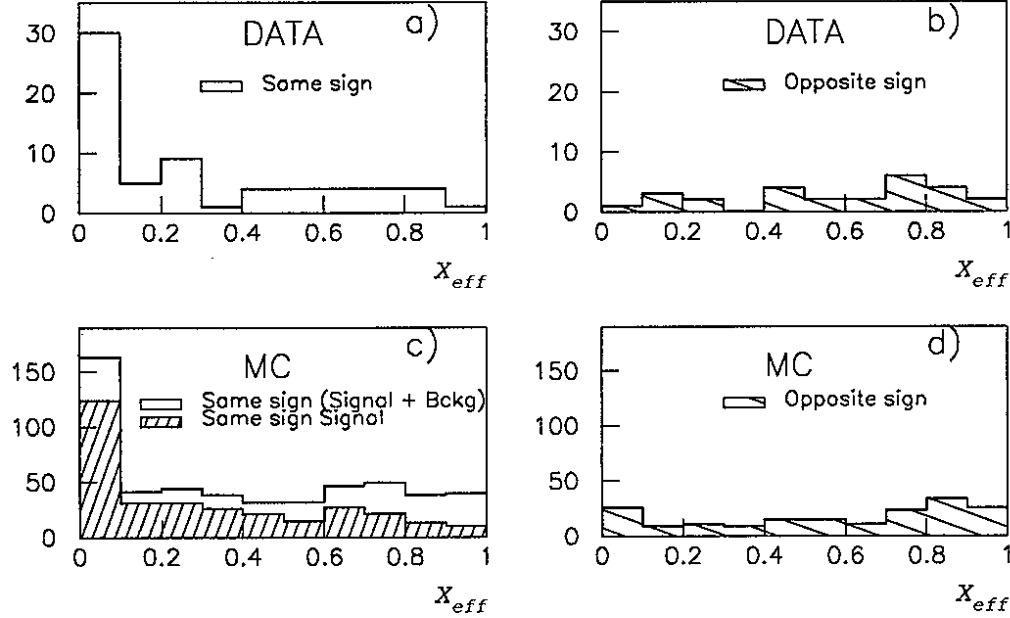


Figure 3: The  $x_{\text{eff}}$  distributions for  $\Xi$ -lepton pairs: (a) and (b) in data, (c) and (d) in simulated events (MC) after all selection cuts described in section 4.2 are applied except the  $\Lambda\pi^-$  mass cut. In (c), the hatched histogram gives the behaviour of  $x_{\text{eff}}$  for the  $\Xi_b$  signal. The MC distributions are not normalised to the data.

Fig. 4 shows the  $\Lambda\pi^-$  invariant mass distribution of the same and opposite sign pairs after the selection cuts (except the  $\Lambda\pi^-$  mass cut), with  $x_{\text{eff}} < 0.3$ . The peak at the  $\Xi^-$  mass is almost completely eliminated from the opposite sign pairs.

The reconstruction efficiency for  $\Xi_b$  signal events leading to  $\Xi^-\ell^-$  pairs, after all selection cuts including  $x_{\text{eff}} < 0.3$ , is estimated from the Monte Carlo simulation to be  $(2.80 \pm 0.15)\%$ , the quoted error being statistical only.

After all the above cuts, taking only the events for which the  $\Lambda\pi$  invariant mass is within the  $\Xi^-$  mass window defined in section 4.2, there are 6  $\Xi^-\ell^+$  pairs and 44  $\Xi^-\ell^-$  pairs, of which 30 are  $\Xi$ -muon and 14 are  $\Xi$ -electron.

## 5 $\Xi_b$ baryon production rate

### 5.1 Background estimation

In order to get the  $\Xi_b$  production rate, one has to estimate the contribution of all  $\Xi$ -lepton pairs coming from sources other than  $\Xi_b$  semileptonic decays. Applying the  $x_{\text{eff}}$  cut on the Monte Carlo sample, it is found that the same sign pairs not coming from  $\Xi_b$  decays are  $1.4 \pm 0.2$  times the number of opposite sign pairs. Applying this same factor to the data, the estimation of the background contribution in the same sign pairs is  $8.4 \pm 3.4$  events.

According to the simulation, the origin of these 8.4 background events may be detailed as follows: 3.5 events come from  $\Lambda_b$  decays, 2.5 events from B meson semileptonic decays, 1 event from the accidental combination between a lepton from a semileptonic B decay and a  $\Xi^-$  from fragmentation, and 1.4 events from the accidental combination between

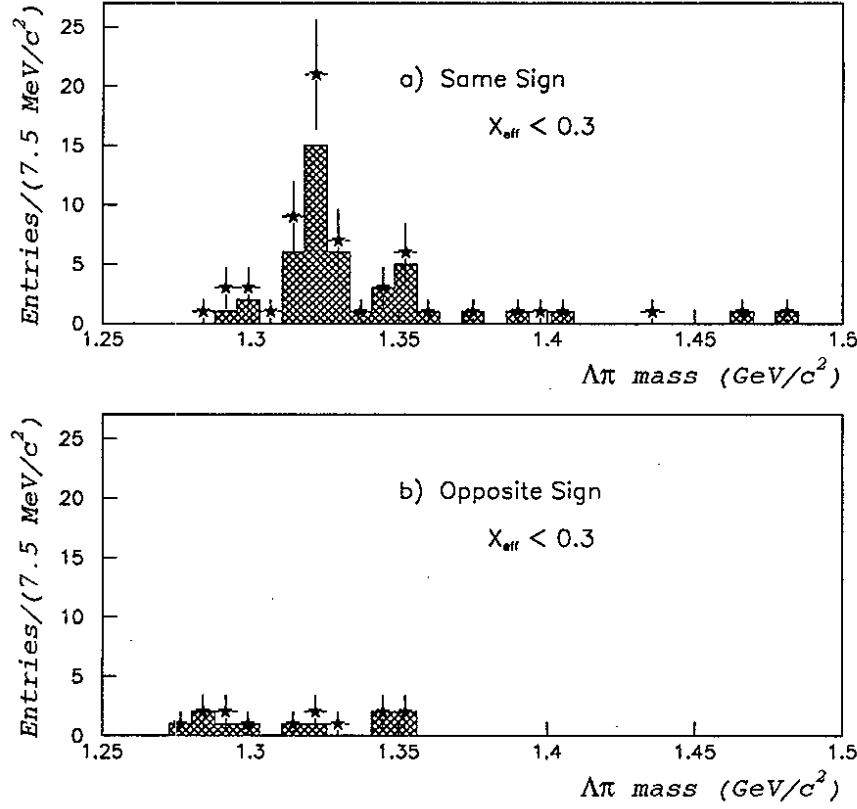


Figure 4: The  $\Lambda\pi^-$  invariant mass distribution of (a) the same sign  $\Xi^-\ell^-$  and (b) the opposite sign  $\Xi^-\ell^+$  combinations after selection cuts and  $x_{\text{eff}} < 0.3$  requirement. The shaded histograms correspond to  $\Xi$ -lepton combinations where the lepton is required to have at least one three-dimensional VDET hit.

the semileptonic decay of a charmed meson or baryon and a  $\Xi^-$  from fragmentation. The contribution from fake combinations is less than 1 event and is neglected.

The background predictions from the Monte Carlo simulation may be considered reliable for processes involving charmed meson or baryon decays, which are fairly well known, and for accidental combinations. The predictions involving b hadrons are less reliable since the measurements are scarce. However two cross-checks can be done.

From the measured decay rate of  $B^0$  and  $B^+$  mesons giving  $\Xi^-$  :

$$\text{Br}(B \rightarrow \Xi^- X) = (2.7 \pm 0.6) \times 10^{-3} [16]$$

and the reconstruction efficiency for this channel (0.3%), a contribution of  $1.5 \pm 0.5$  events to the  $\Xi^-\ell^-$  spectrum is expected. The  $B_s$  decay to  $\Xi^-$  is not measured; using the reconstruction efficiency for this channel (0.5%), and taking a decay rate 3 times higher than for  $B^+$  or  $B^0$ , as suggested by the Monte Carlo, gives a  $B_s$  contribution of  $0.7 \pm 0.2$  events. The total estimation of  $2.2 \pm 0.5$  events coming from B semileptonic decays is consistent with the Monte Carlo expectation given above.

The  $\Lambda_b$  branching ratios are presently poorly known experimentally. Using the measured values:

$$\text{Br}(b \rightarrow \Lambda_b) \times \text{Br}(\Lambda_b \rightarrow \Lambda_c^+ \ell^- \bar{\nu}) = (1.51 \pm 0.37) \times 10^{-2} [17]$$

$$\text{Br}(\Lambda_c^+ \rightarrow \Xi^- K^+ \pi^+) = (3.8 \pm 1.2) \times 10^{-3} [18]$$

and the reconstruction efficiency for this channel (1.2%), a contribution of  $0.8 \pm 0.3$  events to the  $\Xi^- \ell^-$  spectrum is expected. One should add the contribution of the four-body channel  $\Lambda_b \rightarrow \Xi_c X \ell^- \bar{\nu}$ ,  $\Xi_c \rightarrow \Xi^- X'$  for which the reconstruction efficiency is 1%; as no measurement is available, the Monte Carlo production rate of  $1.2 \times 10^{-4}$  is taken, leading to a contribution of  $1.5 \pm 0.4$  events. These two  $\Lambda_b$  decay channels yield an estimated contribution of  $2.3 \pm 0.5$  events.

There is no evident contradiction between the predictions of the Monte Carlo simulation and the rates calculated from available measurements. However, as the  $\Lambda_b$  contribution is the less well known experimentally, the prediction of 3.5 events coming from  $\Lambda_b$  decays will be considered as known with 100% uncertainty in the estimation of systematic errors.

Therefore the estimate of the number of background events in the  $\Xi^- \ell^-$  data sample is  $8.4 \pm 3.4(\text{stat}) \pm 3.5(\text{syst})$ . The probability that this number fluctuates to give the 44 observed events or more is negligibly small.

## 5.2 Production rate

From the above discussion, the number of  $\Xi$ -lepton pairs coming from  $\Xi_b$  decays after selection cuts is  $N(\Xi_b \rightarrow \Xi^- \ell^-) = (35.6 \pm 7.5)$  events.

Taking into account the  $\Lambda \rightarrow p \pi^-$  branching ratio [13] and using the measured fraction of Z decays to  $b\bar{b}$  relative to all Z hadronic decays,  $R_b = 0.2206 \pm 0.0021$  [19], the production rate of  $\Xi_b$  baryons decaying into same sign  $\Xi^- \ell^-$  pairs is:

$$\text{Br}(b \rightarrow \Xi_b) \text{Br}(\Xi_b \rightarrow X_c X \ell^- \bar{\nu}) \text{Br}(X_c \rightarrow \Xi^- X') = (5.4 \pm 1.1(\text{stat}) \pm 0.8(\text{syst})) 10^{-4}$$

per lepton species, averaged over electrons and muons. This result is consistent with the one given in [6].

Table 1: Contributions to the systematic uncertainty in the  $\Xi_b$  production rate.

Source of uncertainty	Uncertainty $\times 10^4$
Contribution of $\Lambda_b$ decays	0.5
$\Xi_b$ decay model	0.4
Reconstruction efficiency	0.3
$x_{\text{eff}}$ cut	0.3
$\Xi_b$ polarisation	0.2
Other	$< 0.1$
Total	0.8

The contributions to the systematic uncertainty are detailed below, and are summarized in Table 1:

- The contribution of  $\Lambda_b$  decays when varied by 100% as described above gives a contribution of  $0.5 \times 10^{-4}$ ;

- A variation in the 4-body semileptonic decay rate of  $\pm 20\%$  is done to estimate the effect of the  $\Xi_b$  decay model: this leads to a contribution of  $0.4 \times 10^{-4}$ ;
- The accuracy on the reconstruction efficiency due to the limited statistics of the Monte Carlo simulation gives a contribution of  $0.3 \times 10^{-4}$ ;
- The production rate has been checked to be stable, within the errors, when varying the  $x_{\text{eff}}$  cut from 0.1 to 0.6; the contribution to the systematic uncertainty is  $0.3 \times 10^{-4}$ . Varying the background fraction  $\eta$  in the definition of  $x_{\text{eff}}$  within its error has a negligible effect on the production rate;
- The effect of a possible  $\Xi_b$  polarisation is small: 100% polarisation gives a variation of 7% in the reconstruction efficiency; however the  $\Xi_b$  are certainly not fully polarised, for instance the  $\Lambda_b$  polarisation has been measured to be around 25% [4]; taking a 50% polarisation for the  $\Xi_b$  gives a contribution of  $0.2 \times 10^{-4}$ .

Other contributions to the systematic uncertainty e.g. the error on  $R_b$  or on the  $\Lambda$  branching ratio are negligible.

## 6 Measurement of the $\Xi_b$ lifetime

### 6.1 Lifetime fit using $\Xi$ -lepton combinations

The final sample of  $\Xi^- \ell^-$  selected events can be used to determine the  $\Xi_b$  lifetime. The method adopted is the one used to measure the  $\Lambda_b$  lifetime from  $\Lambda$ -lepton combinations [17]. Only the important points of this method are given below.

The lepton is required to have one three-dimensional hit in at least one of the VDET layers. This implies that only data with the vertex detector in good operating conditions are used for the lifetime measurement; this restricts the data sample to 3.93 million hadronic Z decays recorded from 1991 to 1995. There are 30  $\Xi^- \ell^-$  and 3  $\Xi^- \ell^+$  events left after the  $x_{\text{eff}} < 0.3$  and VDET requirements (shaded histograms in Fig. 4).

The lifetime is determined by a maximum likelihood fit to the impact parameter distribution of the leptons belonging to the  $\Xi^- \ell^-$  sample. The impact parameter is calculated in the plane perpendicular to the beam axis ( $r$ - $\phi$  plane), as the closest approach of the track to the interaction point. Then, the sign of the projection on the expected  $\Xi_b$  direction (approximated by the jet axis) is given to the impact parameter.

The experimental impact parameter distribution used to perform the fit is obtained by the convolution of the resolution function, describing the detector smearing and the error on the position of the primary vertex, with a “physics function” which is the expected signed impact parameter distribution without resolution effects. This physics function is obtained from the Monte Carlo simulation and may depend on the b quark fragmentation and  $\Xi_b$  decay models.

Five sources of leptons are considered in the fit:

- semileptonic decays of the  $\Xi_b$  baryons (“the signal”), with the unknown lifetime as a free parameter in the fit;
- semileptonic decays of the  $\Lambda_b$  baryon in the decay channels  $\Lambda_b \rightarrow X_c X \ell^- \bar{\nu}_\ell$ , followed by  $X_c \rightarrow \Xi^- X$ ;
- semileptonic decays of B mesons giving a  $\Xi^-$  and a lepton;

- leptons from accidental correlations between a  $\Xi^-$  from fragmentation and a lepton from the semileptonic decay of a b meson or baryon;
- leptons from accidental correlations between a  $\Xi^-$  from fragmentation and a lepton from the semileptonic decay of a c meson or baryon.

The contribution of fake combinations is small enough to be neglected in the fit.

The overall background contribution is estimated from the 3 opposite sign events in the data, corrected by the background asymmetry factor of 1.4 defined in section 5.1. This gives  $4.2 \pm 2.4$  events, which is  $(14 \pm 8)\%$  of the total. Table 2 shows the individual fractions for each background channel.

Table 2: Background contributions to the lifetime fit. The D meson lifetime is a weighted average of the  $D^0$ ,  $D^+$  and  $D_s$  lifetimes.

Background channel	Background fraction %	Average lifetime (ps)	References for lifetimes
$b \rightarrow \Lambda_b \rightarrow \ell \Xi$	6.0	$1.20 \pm 0.20$	[20]
$b \rightarrow B \rightarrow \ell \Xi$	4.0	$1.55 \pm 0.10$	[21],[22]
$c \rightarrow D \rightarrow \ell, \Xi$ fragmentation	2.5	$0.65 \pm 0.05$	[13]
$b \rightarrow B \rightarrow \ell, \Xi$ fragmentation	1.5	$1.55 \pm 0.10$	[21],[22]

The resolution functions (described by two Gaussians) are those used for the  $\Lambda_b$  lifetime determination in  $\Lambda$ -lepton combinations [17], with the same error rescaling factor of 1.3 on the data sample to account for the differences with the Monte Carlo error simulation.

The “physics functions” are parameterised for each lepton source by the use of one exponential for the negative values of the impact parameter and two exponentials for the positive values.

The unbinned maximum likelihood fit to the signed lepton impact parameter distribution for the 30  $\Xi^- \ell^-$  events yields the  $\Xi_b$  lifetime :

$$\tau_{\Xi_b} = 1.35^{+0.37}_{-0.28}(\text{stat}) \text{ ps}$$

Fig. 5 shows the measured impact parameter distribution, together with the result of the fit and the contribution of the background.

## 6.2 Systematic uncertainties

The contributions from the main sources of systematic uncertainties affecting the present measurement are investigated and their respective contributions are summarized in Table 3.

**Resolution function:** the resolution function has been changed within the statistical error of its parametrisation, and the rescaling factor of 1.3 applied for the data has been varied from 1.0 to 1.7. This gives a systematic uncertainty of  $\pm 0.10$  ps to the lifetime.

**Impact parameter:** in the data, the occurrence of large impact parameter events ( $\delta > 0.1$  cm) is higher than in the Monte Carlo sample. To take this effect into account,

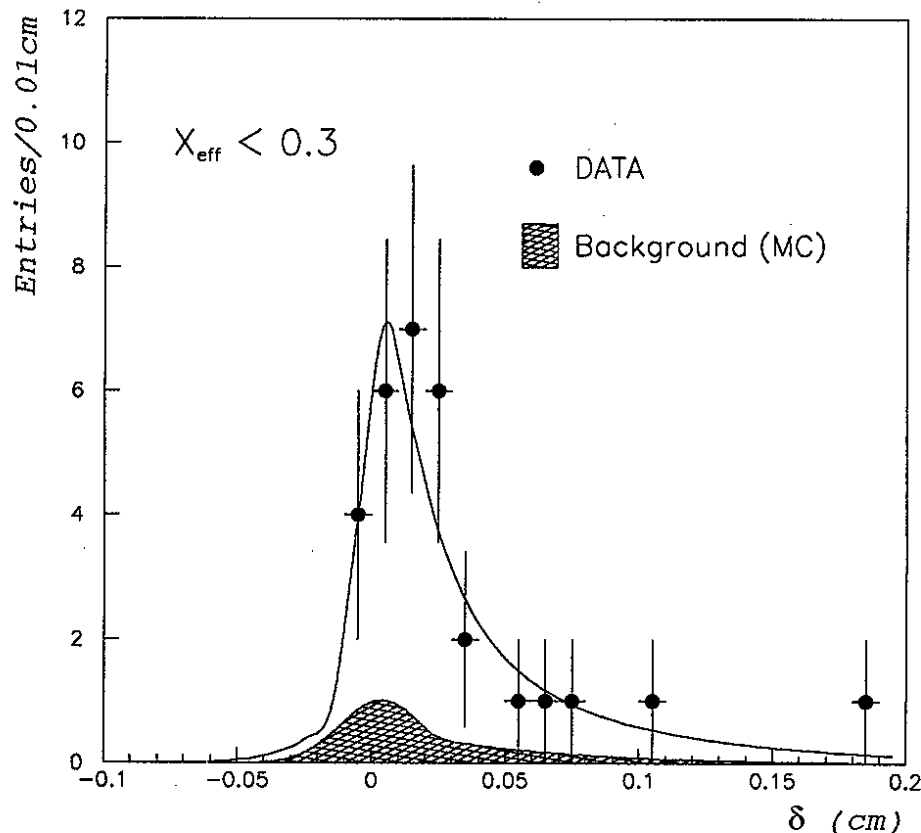


Figure 5: Impact parameter distribution of the selected  $\Xi^-\ell^-$  events. The solid line is the result of the maximum likelihood fit.

the lifetime fit has been tried with a modified version of the resolution functions including a third Gaussian with a much larger resolution. This leads to a systematic uncertainty of  $^{+0.00}_{-0.08}$  ps in the lifetime determination.

**Overall background rate:** the overall background contribution has been varied within its 60% relative uncertainty; this gives a  $\pm 0.05$  ps variation on the lifetime.

**Background composition:** varying the background components within their statistical error gives a  $\pm 0.05$  ps variation of the lifetime. The effect of the errors on the lifetimes of the different background components is negligible.

**Physics function:** the uncertainty in the parametrisation of the physics functions is due to the limited Monte Carlo statistics and leads to a systematic uncertainty of  $\pm 0.05$  ps on the lifetime measurement.

**Effect of the  $x_{\text{eff}}$  cut:** The lifetime measurement has been checked to be stable, within the errors, when varying the  $x_{\text{eff}}$  cut from 0.1 to 0.6; the contribution to the systematic error on the lifetime is  $\pm 0.05$  ps.

**Effect of  $\Xi_b$  polarisation:** The fit has been done on the two Monte Carlo “signal” samples generated with 100% polarisation and no polarisation. The difference on the fitted lifetime between these two extreme cases is 0.04 ps. Assuming a 50% polarisation for the  $\Xi_b$  gives a  $\pm 0.02$  ps variation on the lifetime.



Table 3: Contributions to the systematic uncertainty in the  $\Xi_b$  lifetime measurement.

Source of uncertainty	Uncertainty (ps)
Resolution function and error estimation	$\pm 0.10$
Impact parameter	$+0.00$ $-0.08$
Overall background rate	$\pm 0.05$
Background composition	$\pm 0.05$
Physics function	$\pm 0.05$
$x_{\text{eff}}$ cut	$\pm 0.05$
$\Xi_b$ polarisation	$\pm 0.02$
$\Xi_b$ decay model	$\pm 0.02$
Other	$\pm 0.05$
Total	$+0.15$ $-0.17$

**Effect of  $\Xi_b$  decay model:** A variation of  $\pm 20\%$  of the proportion of 4-body decays, as already used in the estimation of systematic effects in the production rate, gives  $\pm 0.02$  ps variation on the lifetime.

The same analysis has been applied to two Monte Carlo samples of  $\Xi_b$  baryons with generated lifetimes of 1.5 and 1.0 ps. The fitted results are  $1.48^{+0.10}_{-0.08}$  ps and  $1.10^{+0.17}_{-0.15}$  ps, respectively, consistent with the input values.

As the  $\Xi_b$  lifetime uncertainty is dominated by the available statistics, other minor sources of systematic errors such as b quark fragmentation are not investigated in detail. From the studies done for the  $\Lambda_b$  lifetime in  $\Lambda$ -lepton combinations [17] they should not exceed 0.05 ps.

The final result for the  $\Xi_b$  lifetime is:

$$\tau_{\Xi_b} = 1.35^{+0.37}_{-0.28}(\text{stat})^{+0.15}_{-0.17}(\text{syst}) \text{ ps.}$$

This value is consistent with the one given in [6].

## 7 Conclusion

A search for events containing a  $\Xi$  baryon and a lepton of the same charge in the same event hemisphere has been performed in a data sample of 4,188,000 hadronic Z decays. An excess of  $35.6 \pm 7.5$  events is found; it is interpreted as evidence for the semileptonic decay of the strange b baryon  $\Xi_b$  and yields the following product branching ratio:

$$\text{Br}(b \rightarrow \Xi_b) \times \text{Br}(\Xi_b \rightarrow X_c X \ell^- \bar{\nu}_l) \times \text{Br}(X_c \rightarrow \Xi^- X') = (5.4 \pm 1.1(\text{stat}) \pm 0.8(\text{syst})) 10^{-4}$$

per lepton species, averaged over electrons and muons.

Using only the events where the lepton has a hit in the silicon vertex detector, an unbinned maximum likelihood fit to the impact parameter distribution of the leptons gives the following

$\Xi_b$  lifetime :

$$\tau_{\Xi_b} = 1.35_{-0.28}^{+0.37}(\text{stat})_{-0.17}^{+0.15}(\text{syst}) \text{ ps.}$$

## Acknowledgements

We wish to thank our colleagues from the accelerator divisions for the successful operation of LEP. We are indebted to the engineers and technicians at CERN and our home institutes for their contribution to the good performance of ALEPH. Those of us from non-member countries thank CERN for its hospitality.

## References

- [1] D. Buskulic *et al.*, (ALEPH Collab.), Phys. Lett. B **359** (1995) 236.
- [2] D. Buskulic *et al.*, (ALEPH Collab.), Phys. Lett. B **278** (1992) 209;  
P. Abreu *et al.*, (DELPHI Collab.), Phys. Lett. B **311** (1993) 379;  
P.D. Acton *et al.*, (OPAL Collab.), Phys. Lett. B **281** (1992) 394.
- [3] D. Buskulic *et al.*, (ALEPH Collab.), Phys. Lett. B **357** (1995) 685;  
P. Abreu *et al.*, (DELPHI Collab.), Phys. Lett. B **311** (1993) 379;  
P.D. Acton *et al.*, (OPAL Collab.), Phys. Lett. B **316** (1993) 435.
- [4] D. Buskulic *et al.*, (ALEPH Collab.), Phys. Lett. B **365** (1995) 437.
- [5] D. Buskulic *et al.*, (ALEPH Collab.), "Measurement of the mass of the  $\Lambda_b$  baryon", preprint CERN-PPE/96-28, to be published in Phys. Lett. B;  
P. Abreu *et al.*, (DELPHI Collab.), "Search for exclusive decays of the  $\Lambda_b$  baryon and measurement of its mass", preprint CERN-PPE/96-16, submitted to Phys. Lett. B.
- [6] P. Abreu *et al.*, (DELPHI Collab.), "Production of strange b baryons decaying into  $\Xi^- \ell^-$  pairs at LEP", preprint CERN-PPE/95-29, submitted to Z. Phys. C.
- [7] D. Decamp *et al.*, (ALEPH Collab.), Nucl. Instrum. and Methods A **294** (1990) 121;  
D. Buskulic *et al.*, (ALEPH Collab.), Nucl. Instrum. and Methods A **360** (1995) 481.
- [8] B. Mours *et al.*, "The design, construction and performance of the ALEPH Silicon vertex Detector", preprint CERN-PPE/96-41, submitted to Nucl. Instrum. and Methods.
- [9] D. Decamp *et al.*, (ALEPH Collab.), Z. Phys. C **53** (1992) 1.
- [10] T. Sjöstrand, Comp. Phys. Com. **82** (1994) 74.
- [11] D. Buskulic *et al.*, (ALEPH Collab.), Nucl. Instrum. and Methods A **346** (1994) 461.
- [12] D. Buskulic *et al.*, (ALEPH Collab.), Z. Phys. C **64** (1994) 361.
- [13] L. Montanet *et al.*, (Particle Data Group), Phys. Rev. D **50** (1994) 1173.

- [14] S. Bethke *et al.*, (JADE Collab.), Phys. Lett. **B 213** (1988) 235.
- [15] D. Buskulic *et al.*, (ALEPH Collab.), "Study of the  $B_s^0 \bar{B}_s^0$  oscillation frequency using  $D_s^- \ell^+$  combinations in Z decays", preprint CERN-PPE/96-30, to be published in Phys. Lett **B**;  
D.E. Jaffe, F. Le Diberder and M.-H. Schune, LAL 94-67 and FSU-SCRI 94-101.
- [16] G. Crawford *et al.*, (CLEO Collab.), Phys. Rev. **D 45** (1992) 752.
- [17] D. Buskulic *et al.*, (ALEPH Collab.), Phys. Lett. **B 357** (1995) 685.
- [18] P. Avery *et al.*, (CLEO Collab.), Phys. Rev. Lett. **71** (1993) 2391.
- [19] The LEP Collaborations ALEPH, DELPHI, L3 and OPAL, "Combining Heavy Flavour Electroweak measurements at LEP", preprint CERN-PPE/96-17, submitted to Nucl. Instrum. and Methods **A**.
- [20] H-G Moser, Review talk on b hadron lifetimes, Proc. of the Int. Europhysics Conference, Brussels, Belgium, August 1995.
- [21] D. Buskulic *et al.*, (ALEPH Collab.), "Improved measurement of the  $\bar{B}^0$  and  $B^-$  meson lifetimes", preprint CERN-PPE/96-14, submitted to Z. Phys. **C**.
- [22] D. Buskulic *et al.*, (ALEPH Collab.), Phys. Lett. **B 361** (1995) 221.